Infrared Spectroscopy of Ozone−Water Complex in a Neon Matrix

Masashi Tsuge,[†] Kazuhide Tsuji,[‡] Akio Kawai,[†] and Kazuhiko Shibuya*,[†]

Department of Chemistry, Graduate School of Science and Engineering, Tokyo Institute of Technology, 2-12-1-H57 Ohokayama, Meguro-ku, Tokyo 152-8551, Japan, and Gunma National College of Technology, 580 Toriba-machi, Maebashi, Gunma 371-8530, Japan

Received: December 5, 2006; In Final Form: January 21, 2007

Matrix isolation infrared spectroscopy has been applied to study an ozone−water complex of atmospheric interest. The complex was identified in the spectral region of three normal modes of ozone and water. Ab initio calculation at MP4(SDQ), QCISD, and CCSD(T) levels indicates the existence of only one stable conformer, which accords with the present experimental result. This conformer belongs to the C_s symmetry group where two molecular planes of ozone and water are perpendicular to the C_s symmetry plane. The binding energy was calculated to be 1.89 kcal/mol at the CCSD(T)/6-311++G(3df,3pd)//CCSD(T)/6-311++G(d,p) level of theory. The formation constant and atmospheric abundance of the ozone−water complex are estimated using the thermodynamic and spectroscopic data obtained.

Introduction

Ozone plays a central role in the chemistry of Earth's atmosphere. The $O(^1D)$ atom is generated in the UV photolysis of ozone and then reacts with H_2O to produce the hydroxyl radical (OH).

$$O_3 + h\nu \rightarrow O(^1D) + O_2 \quad (1)$$

$$O(^1D) + H_2O \rightarrow 2OH \quad (2)$$

The UV light below 340 nm is thought to be important in the $O(^1D)$ production from an ozone monomer in the atmosphere.[1] The hydroxyl radical is one of the most important oxidants (OH, O_3, NO_3) in the atmosphere: specifically, OH and O_3 take on the leading role in the daytime chemistry. Recently, the ozone−water complex, O_3-H_2O, has been proposed to be a possible source for the hydroxyl radical in the troposphere. According to the estimate by Frost and Vaida,[2] 0.001−0.01% of tropospheric ozone exists as a water complex form. The complex formation has a possibility of model change in the photochemical mechanism related to ozone. The hydroxyl radical might be produced efficiently through the photolysis of the O_3-H_2O complex.[3−5] The work of Hurwitz and Naaman[4] showed that the quantum yield of the hydroxyl radical through the 355 nm photolysis of the ozone−water complex was 1% of that of the 266 nm photolysis, whereas the absorption coefficient of the ozone monomer at 355 nm is 0.01% that of 266 nm. Therefore, upon the water complex formation, the product of the absorption coefficient and $O(^1D)$ quantum yield might increase by 2 orders of magnitude. The more accurate estimation for the abundance of the complex is required to improve the atmospheric reaction model. Information on the binding energy and rotational/vibrational structure of the O_3-H_2O complex are required for it.

The binding energy of the O_3-H_2O complex has been calculated and reported by a few papers.[6−8] Gillies et al.[7] recorded the microwave spectrum of the ozone−water complex and determined its configuration to be of C_s symmetry with three atoms of water and a center oxygen of ozone lying on the symmetry plane. This plane bisects the O−O−O angle of ozone. They also performed an ab initio calculation at the MP2/6-31G(d,p) and MP4(SDTQ)/6-31G(d,p) levels of theory and reported the calculated binding energies ranging from 0.7 to 2.4 kcal/mol. More recently, Tachikawa and Abe[8] have carried out a QCISD calculation and concluded that the complex has three stable conformers. One, which is called "dipole", has the configuration similar to one Gillies et al. proposed, and the other two, "cis" and "trans", have hydrogen-bonded configurations. The binding energies of three "dipole", "cis", and "trans" isomers were calculated to be 2.39, 2.27, and 2.30 kcal/mol, respectively, at the QCISD(T)/6-311++G(3df,3pd)//QCISD/6-311++G(d,p) level of theory. From a comparison of experimental and calculated rotational constants, they concluded that the "dipole" conformer was a probable candidate for the experimentally observed the O_3-H_2O complex.

The vibrational frequencies of ozone monomer and its dimer in cryogenic matrices have been well-investigated.[9,10] The IR studies of O_3-molecule complexes have been reported on various molecular systems such as CO, NO, NO_2, and H_2O.[11−13] There has been only one report on the vibrational frequencies of the O_3-H_2O complex. Schriver et al.[13] prepared the complex in an argon matrix and recorded the infrared absorption spectrum. They assigned 1:1, 2:1, and 1:2 complexes of ozone and water. By comparing it with the SO_2-H_2O case, where the intermolecular bond was formed between a sulfur atom and water oxygen, they concluded that the O_3-H_2O 1:1 complex had a hydrogen-bonded configuration. The binding energy of the O_3-H_2O complex was postulated to be less than 1 kcal/mol from the frequency shift of water symmetric stretching vibration. Unfortunately, the complex bands in the ozone fundamental regions were not fully resolved from ozone monomer and dimer bands because of a higher concentration of ozone, O_3/Ar = 1/100, and a spectral resolution of approximately 0.5 cm^{-1}.

* Corresponding author. E-mail: kshibuya@chem.titech.ac.jp. Phone and Fax: (+81)-3-5734-2224.
[†] Tokyo Institute of Technology.
[‡] Gunma National College of Technology.

10.1021/jp068364m CCC: $37.00
Published on Web 04/19/2007

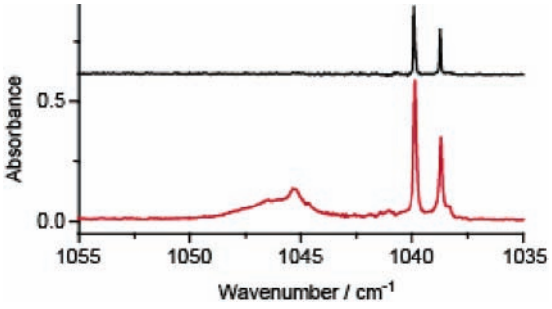

Figure 1. IR absorption spectra in the ozone asymmetric stretching frequency region: (upper) O_3/Ne = 1/4000, (lower) O_3/H_2O/Ne = 1/5/4000. Spectra were recorded at 6 K with a spectral resolution of 0.0625 cm^{-1}.

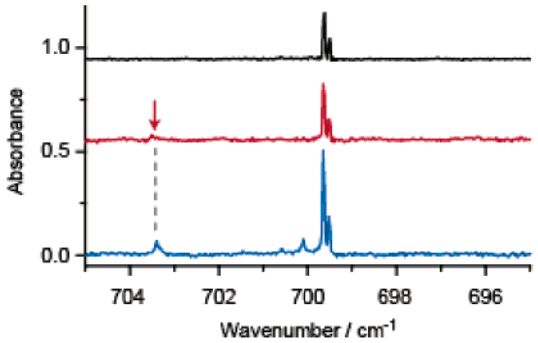

Figure 2. IR absorption spectra in the ozone bending frequency region: (upper) O_3/Ne = 1/4000, (middle) O_3/H_2O/Ne = 1/5/4000, (lower) O_3/H_2O/Ne = 5/5/4000. Spectra were recorded at 6 K with a spectral resolution of 0.0625 cm^{-1}. A vertical arrow indicates the absorption of the ozone−water complex. A band at 700.1 cm^{-1} in the lower trace is due to an impurity.

The principal aim of this study is to determine the precise vibrational frequency of the O_3-H_2O complex. We employed neon as the matrix medium to reduce a frequency shift from the gas-phase value. In the frequency regions of three fundamental vibrations of ozone and water, we identified vibrational bands due to the ozone−water complex by studying the concentration and isotope effects on the infrared spectra. We carried out a high level ab initio calculation to determine stable conformer and unstable transition state configurations of the O_3-H_2O complex. The observed and calculated frequency shifts upon the complexation are determined. On the basis of the calculated binding energy, we estimate the equilibrium constant for the complexation.

Experiment and Calculation

An ozone sample was stored in a silica gel trap at approximately 200 K after passing an O_3-containing gas mixture from a commercial ozonizer. Mixture of O_3/Ne, O_3/H_2O/Ne, and O_3/D_2O (Acros Organics, 100.0 atom % D)/Ne with various mixing ratios were prepared by standard manometric techniques. Gas samples were deposited onto a CsI plate maintained at ~6 K using a closed-cycle helium refrigerator (Iwatani Industrial Gases Corp., CryoMini). The typical deposition rate was ~10 mmol/h. The vacuum lines made of stainless steel were heated enough before deposition to eliminate trace amounts of water, which was especially important for the O_3/Ne experiments. The infrared spectra of 0.25 or 0.0625 cm^{-1} resolution were recorded by using an FTIR spectrometer (JEOL, SPX200) equipped with a liquid nitrogen-cooled microchannel plate detector. The entire optical path was purged by N_2 gas to avoid the atmospheric absorption of H_2O and CO_2.

Ab initio calculations were performed using the Gaussian 03 package.[14] Geometry optimization were performed at the MP4(SDQ), QCISD, and CCSD(T) levels with the 6-311++G(d,p) and 6-311++G(3df,3pd) basis sets. The binding energy of the ozone−water complex was calculated at the QCISD(T)/6-311++G(3df,3pd)//QCISD/6-311++G(d,p), CCSD(T)/6-311++G(d,p), and CCSD(T)/6-311++G(3df,3pd)//CCSD(T)/6-311++G(d,p) levels of theory. The basis set superposition error was corrected by the counterpoise correction.[15] The vibrational frequency calculations at the optimized geometries were performed at the MP4(SDQ)/6-311++G(d,p), QCISD/6-311++G(d,p), and CCSD(T)/6-311++G(d,p) levels of theory.

Results and Discussion

FTIR Spectra in Ozone ν_1-, ν_2-, and ν_3-Frequency Regions. Figure 1 shows the FTIR spectra of O_3/Ne (upper trace) and O_3/H_2O/Ne (lower trace) in the ozone asymmetric stretching (ν_3) frequency region. In the upper trace for the O_3/Ne (= 1/4000) sample, the ν_3 mode was observed as a doublet peaking at 1038.7 and 1039.9 cm^{-1}, whose line widths (full width at half-maximum, fwhm) were less than 0.1 cm^{-1}. This coincides with the previously reported observation.[10] The doublet is thought to be due to the matrix site effect. During warming up to 10 K, the 1038.7 cm^{-1} band blue shifts, while the 1039.9 cm^{-1} band becomes narrower. On the basis of the well-characterized result for the argon matrix isolated OCS molecule,[16,17] we tentatively assigned the 1038.7 and 1039.9 cm^{-1} bands to the ν_3 bands of the ozone monomer isolated in the meta-stable and stable sites, respectively. As shown in the lower trace for the O_3/H_2O/Ne (= 1/5/4000) sample, a new broad band appears at 1043−1049 cm^{-1} (the 1045 cm^{-1} band). This band would be assigned because of the $O_3-(H_2O)_n$ complex. In the infrared spectrum for a sample with a higher H_2O concentration (O_3/H_2O/Ne = 1/20/4000, not shown in figures), the relative intensity of the 1045 cm^{-1} band to the ozone monomer bands becomes stronger without a large change in the band shape, and no additional bands appear. This observation may indicate that the $O_3-(H_2O)_n$ ($n \geq 2$) complexes are not likely to be formed in a neon matrix.

Figure 2 shows the FTIR spectra of O_3/Ne = 1/4000 (upper trace), O_3/H_2O/Ne = 1/5/4000 (middle trace), and O_3/H_2O/Ne = 5/5/4000 (lower trace) in the ozone bending (ν_2) frequency region. The ν_2 mode of the ozone monomer was observed as a doublet structure at 699.4 and 699.5 cm^{-1}. Infrared absorption at 703.4 cm^{-1} will be due to the O_3-H_2O complex. Similarly in the ozone ν_3 region, the spectrum obtained in an O_3/H_2O/Ne mixture with a higher H_2O concentration did not show any additional band.

Figure 3 shows the FTIR spectra of O_3/Ne (upper trace) and O_3/H_2O/Ne (lower trace) in the ozone symmetric stretching (ν_1) frequency region. The ν_1 mode of the ozone monomer was observed very weakly at 1104.4 and 1103.4 cm^{-1}. The relative intensities of these bands to the ozone asymmetric stretching band are less than 1/200 in a neon matrix, which is smaller than the corresponding ratio in the gas phase. As shown in the lower trace, the infrared absorption possibly due to the O_3-H_2O complex was observed at 1108−1115 cm^{-1} (the 1110 cm^{-1} band).

FTIR Spectra in a Water (H_2O, D_2O, and HDO) ν_2-Frequency Region. The assignments for the rovibrational bands of the water monomer and its dimer in a neon matrix have been reported by Forney et al.[18] Figure 4 shows the FTIR spectra in the bending (ν_2) frequency regions for (a) H_2O, (b) D_2O, and (c) HDO. The FTIR spectra of water/Ne with the ratio of 5/4000

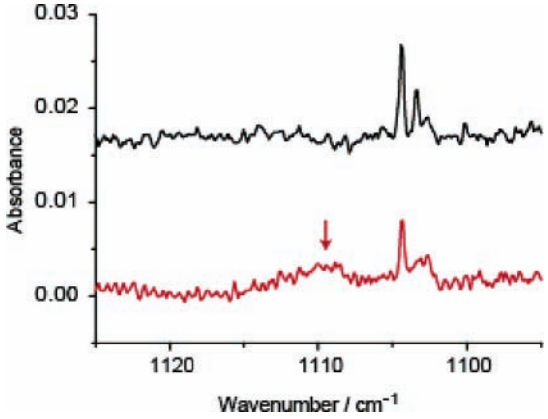

Figure 3. IR absorption spectra in the ozone symmetric stretching frequency region: (upper) O_3/Ne = 1/4000, (lower) O_3/H_2O/Ne = 10/5/4000. Spectra were recorded at 6 K with a spectral resolution of 0.25 cm^{-1}. A vertical arrow indicates the absorption of the ozone−water complex.

are shown in the upper traces as reference. The lower traces in Figure 4a−c were taken for the samples of O_3/H_2O/Ne = 1/5/4000, O_3/D_2O/Ne = 1/5/4000, and $O_3/(H_2O + D_2O + HDO)$/Ne = 1/5/4000, respectively. When we compare the upper and lower traces of Figure 4a, it turns out that the 1598.3 cm^{-1} band was observed only for the sample containing both O_3 and H_2O. This band was found to lie between the 1595.6 and 1599.2 cm^{-1} bands assigned to the H_2O nonrotating monomer (NRM) and the proton-acceptor band of $(H_2O)_2$, respectively, where the NRM band of H_2O corresponds to a rovibrational band of $0_{0,0}-0_{0,0}$ transition. This result indicates that the O_3-H_2O complex is not formed through a strong hydrogen bond. For example, the proton-donor band of $(H_2O)_2$ in a neon matrix is reported to be located at 1616.5 cm^{-1},[19] being blue shifted by 20.9 cm^{-1} from the NRM band. In Figure 4b, a 1180.6 cm^{-1} band was observed only for the sample containing both O_3 and D_2O. This band also lies between the D_2O NRM band at 1178.7 cm^{-1} and the deuteron-acceptor band of $(D_2O)_2$ at 1181.6 cm^{-1}. In the HDO region shown in Figure 4c, a 1405.9 cm^{-1} band was observed only for the mixture containing all of the O_3, H_2O, D_2O, and HDO. This band, again, lies between the HDO NRM band at 1404.1 cm^{-1} and an acceptor band of $(HDO)_2$ at 1408.0 cm^{-1}.

Similarly, as described above, we could identify additional three bands of O_3-D_2O and O_3-HDO in the spectral regions of the symmetric (ν_1) and asymmetric (ν_3) stretchings of the corresponding isotopic water moiety. The 2672.3 and 2782 cm^{-1} bands are due to the D_2O ν_1 and ν_3 bands within the O_3-D_2O complex, respectively, and the 2715.3 cm^{-1} band is attributed to the HDO ν_1 band within the O_3-HDO complex (Figure 1S, Supporting Information). These three bands were observed to be blue shifted from the corresponding water−monomer NRM bands upon the complexation. We could not identify the H_2O ν_1 and ν_3 bands within the O_3-H_2O complex and the HDO ν_3 band within the O_3-HDO complex. Possibly, the other bands of the water moiety within the ozone−water complexes overlap with the corresponding IR bands of the water monomer or the dimer.

Geometrical Configuration and Binding Energy of the Ozone−Water Complex. First, the stable configuration of the O_3-H_2O complex was calculated at the MP4(SDQ)/6-311++G(d,p) and QCISD/6-311++G(d,p) levels of theory. The optimization was performed from a variety of initial configurations including three isomers of "dipole", "cis", and "trans" reported by Tachikawa and Abe.[8] The SCF convergence criteria for

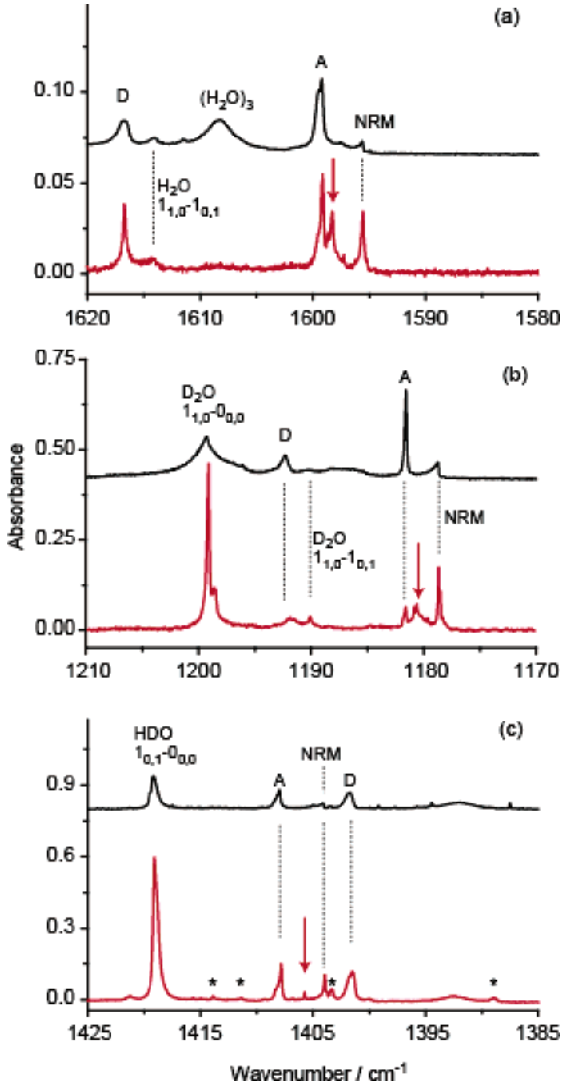

Figure 4. IR absorption spectra in the bending frequency regions of water (H_2O, D_2O, and HDO): (a) O_3/H_2O/Ne = 1/5/4000, (b) O_3/D_2O/Ne = 1/5/4000, and (c) $O_3/(H_2O + D_2O + HDO)$/Ne = 1/5/4000. The FTIR spectra of water/Ne with the ratio of 5/4000 are shown in the upper traces as reference. Spectra were recorded at 6 K with a spectral resolution of 0.0625 cm^{-1}. Vertical arrows indicate the absorption due to the ozone−water complex. D and A indicate proton-donor and proton-acceptor bands, respectively, of the water dimer. NRM corresponds to a nonrotating water monomer. Bands marked with an asterisk (*) are due to an impurity, unassigned water bands, or both.

optimization were achieved at four configurations of "double-decker", "dipole", "cis", and "trans". The "double-decker" conformer is illustrated in Figure 5. In this conformer, each moiety of O_3 and H_2O remains C_{2v} symmetry. This conformer has C_s symmetry with the center oxygen atom of ozone (the position number of 2) and the oxygen atom of water (the position number of 4) lying on the symmetry plane. The optimized geometrical parameters are summarized in Table 1. The other configurations are illustrated in Figure 6. Parameters for the "dipole", "cis", and "trans" are essentially the same with those reported by Tachikawa and Abe. To confirm the stability of the configuration, we performed a harmonic frequency analysis at the QCISD/6-311++G(d,p) level of theory. It was only one "double-decker" conformer in many optimized configurations to give real frequencies for all of the normal modes. Calculated frequencies are summarized in Table 2, and approximate representations of intermolecular modes are shown in Figure 7. For the "double-decker" conformer, the geometry

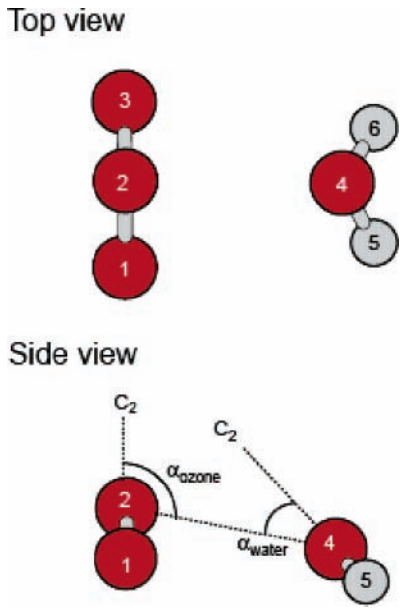

Figure 5. Stable "double-decker" conformer of the ozone−water complex optimized at the CCSD(T)/6-311++G(d,p) level of theory. Geometric parameters of α_{ozone} and α_{water} are defined as the angles made by a line connecting center oxygens of O_3 (2) and H_2O (4) and the C_2 axes of O_3 and H_2O moieties, respectively.

TABLE 1: Geometrical Parameters Optimized for the O_3-H_2O "double-decker" Complex[a]

	MP4(SDQ)	QCISD	CCSD(T)	CCSD(T)with CP[b]
r_{12} (= r_{23})	1.2494	1.2536	1.2735	1.2738
r_{45} (= r_{46})	0.9589	0.9591	0.9608	0.9603
r_{24}	2.8583	2.8613	2.8661	3.0020
θ_{123}	118.0	117.8	117.0	117.1
θ_{546}	103.8	103.8	103.5	103.6
α_{ozone}	95.6	95.0	94.5	97
α_{water}	32.2	32.5	27.8	26.2

[a] 6-311++G(d,p) basis set was used. Bond lengths (r_{ij}) and angles (θ_{ijk}, α) are in angstroms and in degrees, respectively. Definition of position numbers (i, j, k), α_{ozone} and α_{water}, are shown in Figure 5. [b] Counterpoise correction was performed.

optimizationwas also performed at the CCSD(T)/6-311++G-(d,p) level of theory. The distance between the center oxygen atom of ozone (the position number of 2) and the oxygen atom of water (the position number of 4) was calculated to be r_{24} = 2.8661 Å.

The calculated energies of selected configurations and intermolecular potentials are shown in Table 3 and Figure 8, respectively. The QCISD(T)/6-311++G(3df,3pd)//QCISD/6-311++G(d,p) calculation with a counterpoise correction for basis set superposition error indicates that the binding energy of the "double-decker" conformer is 1.86 kcal/mol, which is larger than those of "dipole" (1.69 kcal/mol), "cis" (1.68 kcal/mol), and "trans" (1.60 kcal/mol) configurations. For the "double-decker" conformer, a more sophisticated calculation of the CCSD(T)/6-311++G(3df,3pd) level with counterpoise correction was performed and gave a binding energy of 1.89 kcal/mol.

For the "double-decker" conformer, we also performed a geometry optimization at the CCSD(T)/6-311++G(d,p) level of theory with a counterpoise corrected potential energy surface. As shown in Table 1, the distance between the center oxygen of ozone (the position number of 2) and the water oxygen (the position number of 4) is r_{24} = 3.0020 Å, which is larger than those calculated at other levels without a counterpoise correction. The binding energy at this geometry was calculated at the

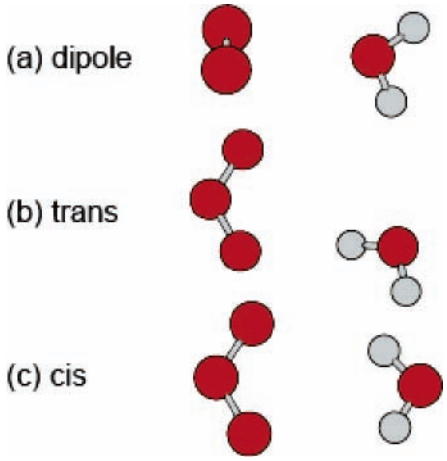

Figure 6. Transition state configurations of the ozone−water complex calculated at the QCISD/6-311++G(d,p) level of theory. The "dipole" configuration has C_s symmetry plane with three atoms of water and center oxygen of ozone in the symmetry plane. All of the atoms of the trans and cis configurations are lying on the C_s symmetry plane.

TABLE 2: Harmonic Vibrational Frequencies Calculated for the O_3-H_2O Complex (Not Scaled, cm^{-1})[a]

		method		
moiety	approximate mode[b]	MP4(SDQ)	QCISD	CCSD(T)
H_2O	antisymmetric stretch (ν_3, A'')	3995	3987	3962
	symmetric stretch (ν_1, A')	3892	3886	3860
	bend (ν_2, A')	1664	1664	1657
O_3	symmetric stretch (ν_1, A')	1298	1251	1152
	antisymmetric stretch (ν_3, A'')	1328	951	1034
	bend (ν_2, A')	773	755	723
inter-molecular	$\nu_1(A')$	203	203	214
	$\nu_4(A'')$	167	159	166
	$\nu_2(A')$	132	131	132
	$\nu_5(A'')$	95	94	93
	$\nu_3(A')$	92	91	90
	$\nu_6(A'')$	65	64	69

[a] 6-311++G(d,p) basis set was used. Geometry optimization and frequency calculations were performed at the same level of theory. [b] Labels of A' and A'' in the parentheses are symmetry species in C_s point group.

CCSD(T)/6-311++G(3df,3pd) level with a counterpoise correction to be 1.89 kcal/mol. This value is the same as one obtained from the geometry which was optimized without a counterpoise correction. This result indicates that the counterpoise correction in an optimization process is not necessarily needed to calculate the binding energy of the O_3-H_2O complex.

As illustrated in Figure 8, the internal rotation along the intermolecular ν_5 mode will transform two "double-decker" conformers via a transition state of the "dipole" configuration. Isomerization along the combination coordinates of intermolecular ν_2, ν_4, and ν_6 modes might connect two "double-decker" conformers via the transition states of "cis" and "trans" configurations. The energy differences between the "double-decker" conformer and the other transition state configurations range from 0.17 kcal/mol of the "dipole" configuration to 0.26 kcal/mol of the "trans" configuration, corresponding from 60 to 90 cm^{-1}, respectively. These values are comparable to the frequencies of intermolecular modes. The ozone−water complex might exist preferentially as the "double-decker"

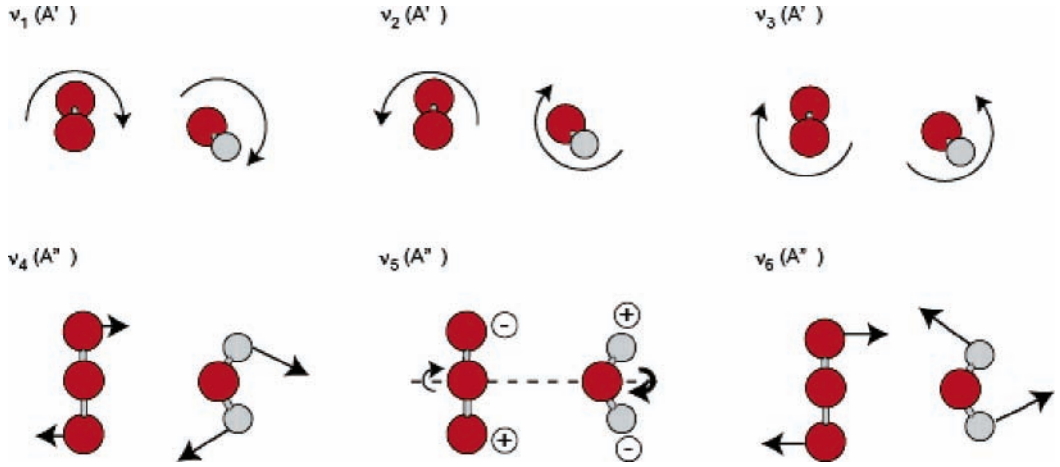

Figure 7. Approximate representations of intermolecular vibrational modes within the O_3-H_2O complex.

TABLE 3: Calculated Energies of the O_3-H_2O Complex Relative to the Sum Energy of O_3 and H_2O Monomers

method		energy (kcal/mol)			
energy calculation[a]	optimization[b]	double decker	dipole[d]	cis[d]	trans[d]
QCISD(T)	QCISD	−2.56	−2.39	−2.27	−2.30
QCISD(T) with CP[c]	QCISD	−1.86	−1.69	−1.68	−1.60
CCSD(T)	CCSD(T)	−2.58			
CCSD(T) with CP[c]	CCSD(T)	−1.89			
CCSD(T) with CP[c]	CCSD(T) with CP[c]	−1.89			

[a] 6-311++G(3df,3pd) basis set was used. [b] 6-311++G(d,p) basis set was used. [c] Basis set superposition errors were corrected by a counterpoise correction. [d] Transition states.

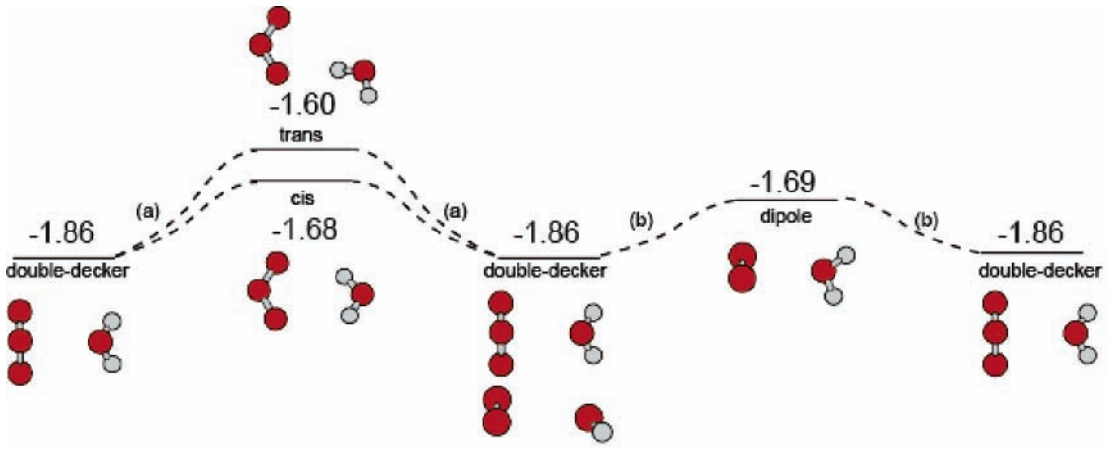

Figure 8. Intermolecular potential of the O_3-H_2O complex calculated at the QCISD(T)/6-311++G(3df,3pd)//QCISD/6-311++G(d,p) level of theory. Counterpoise corrected energies (kcal/mol) relative to the sum energy of O_3 and H_2O monomers are given. (a) Isomerization along the combination coordinates of intermolecular ν_2, ν_4, and ν_6 modes. (b) Internal rotation along the intermolecular ν_5 mode.

conformer at 6 K, but the isomerizations are likely to occur easily at atmospheric temperatures.

The rotational constants of the O_3-H_2O complex in the double-decker conformer calculated at the CCSD(T)/6-311++G(d,p) level of theory with a counterpoise correction are $A = 11.5357$, $B = 4.0472$, and $C = 3.1806$ GHz, which are different from the experimental values of $A = 11.9606$, $B = 4.1740$, and $C = 3.2652$ GHz derived from the microwave spectrum.[7] The agreement between calculation and experiment does not seem good, also for the similar flexible complex like HO_2-H_2O: The microwave spectrum gives the constants of $A = 32.897$, $B = 5.656$, and $C = 4.829$ GHz, while the ab initio calculation leads to the values of $A = 31.806$, $B = 5.968$, and $C = 5.077$ GHz.[20]

The configuration expected from the microwave data is similar to the "dipole" configuration;[7] this expectation conflicts with the present calculation which predicts that the "dipole" configuration corresponds to the transition state. This kind of discrepancy has been reported for another flexible complex of O_2-H_2O.[21] The microwave spectrum indicated that the O_2-H_2O complex has a C_{2v} structure (the $\bar{B}$ constant of 3.633 GHz), while the calculation leads to two asymmetric C_s structures (the $\bar{B}$ constant of 4.092 GHz). This discrepancy between microwave data and equilibrium geometry has been reasonably understood in terms of the low-frequency vibration of O_2-H_2O: The large amplitude vibration between two equivalent minima with asymmetric C_s symmetry gives an apparent symmetric C_{2v} structure as the averaged geometry. Actually, the symmetric C_{2v} structure corresponds to a transition state connecting two equivalent minima with asymmetric C_s symmetry.[22] For the present O_3-H_2O complex, the isomerization barriers through the transition states are also as low as the frequencies of intermolecular vibration, and therefore the complex will isomer-

TABLE 4: Vibrational Frequencies of the O_3-H_2O Complex (cm^{-1})

		obs in Ne matrix			calcd[d]		
moiety	approximate mode	monomer	complex	$\Delta\nu$[c]	monomer	complex	$\Delta\nu$[c]
O_3	symmetric stretch (ν_1)	1104.4 1103.4	1110	+5.6	1140	1152	+12
	(i) antisymmetric stretch (ν_3)	1039.9 1038.7	1045.3	+5.4	1016	1034	+18
	bend (ν_2)	699.5 699.4	703.4	+3.9	718	723	+5
	$\nu_1+\nu_3$	2109.9 2107.6	2119.8	+9.9			
H_2O	antisymmetric stretch (ν_3)	3750.7[a]	n.d.[b]		3971	3962	−9
	symmetric stretch (ν_1)	3660.6[a]	n.d.[b]		3867	3860	−7
	(ii) bend (ν_2)	1595.6[a]	1598.3	+2.7	1644	1657	+13

[a] Taken from ref 18. [b] Frequencies are not determined from the experiments possibly because of overlapping. [c] Calculated by $\Delta\nu = \nu_{complex} - \nu_{monomer}$. [d] CCSD(T)/6-311++G(d,p), not scaled.

TABLE 5: Vibrational Frequencies of O_3-D_2O and O_3-HDO Complexes (cm^{-1})[a]

		obs in Ne matrix			calcd[e]		
moiety	approximate mode	monomer[b]	complex	$\Delta\nu$[d]	monomer	complex	$\Delta\nu$[d]
D_2O	antisymmetric stretch (ν_3)	2787	2782	−5	2908	2902	−6
	symmetric stretch (ν_1)	2672.7	2672.3	−0.4	2789	2784	−5
	bend (ν_2)	1178.7	1180.6	+1.9	1203	1212	+9
HDO	antisymmetric stretch (ν_3)	3699	n.d.[c]		3921	3912	−9
	symmetric stretch (ν_1)	2722.9	2715.3	−8	2847	2841	−6
	bend (ν_2)	1404.1	1405.9	+1.8	1440	1452	+12

[a] Frequency shifts of ozone fundamentals are essentially the same with those within the O_3-H_2O complex listed in Table 4. [b] Taken from ref 18. [c] Frequency is not determined from the experiments possibly because of overlapping. [d] Calculated by $\Delta\nu = \nu_{complex} - \nu_{monomer}$. [e] CCSD(T)/6-311++G(d,p), not scaled.

ize easily. Large amplitude motions or intra-complex low-frequency vibration on a global potential energy surface will give an apparent/averaged geometry of O_3-H_2O, which may explain the discrepancy between results derived from the microwave experiment and the ab initio calculation.

Comparison of the Experimental and Calculated Vibrational Frequencies. Vibrational frequencies of the ozone−water complex were calculated at the MP4(SDQ), QCISD, and CCSD(T)/6-311++G(d,p) levels of theory. The asymmetric stretching (ν_3) frequencies of the ozone monomer were calculated to be 1324, 934, and 1016 cm^{-1} at the MP4(SDQ), QCISD, and CCSD(T) level, respectively. The band origin of this vibration in the gas phase has been reported to be 1042 cm^{-1}.[23] The CCSD(T) level calculation seems to estimate the vibrational frequency of ozone reasonably well. Thus, we have adopted vibrational frequencies calculated at the CCSD(T)/6-311++G(d,p) level of theory.

The observed and calculated frequencies of the O_3-H_2O complex are listed in Table 4, together with the frequency shifts upon the complexation. By forming the water complex, all of the normal frequencies of ozone are calculated to blue shift ($\Delta\nu > 0$). The calculated frequency shifts ($\Delta\nu_1 = +12$ cm^{-1}, $\Delta\nu_2 = +5$ cm^{-1}, and $\Delta\nu_3 = +18$ cm^{-1}) correspond to the observed shifts ($\Delta\nu_1 = +6$ cm^{-1}, $\Delta\nu_2 = +4$ cm^{-1}, and $\Delta\nu_3 = +5$ cm^{-1}) for the vibrations of the ozone moiety. For the water moiety, the calculation indicates that the symmetric and asymmetric stretching frequencies red shift ($\Delta\nu_1 = -7$ cm^{-1}, $\Delta\nu_3 = -9$ cm^{-1}), the bending blue shifts ($\Delta\nu_2 = +13$ cm^{-1}). We could not identify the water ν_1 and ν_3 bands within the O_3-H_2O complex, possibly because of an overlapping with the water monomer, multimer, or both bands.

The frequencies and frequency shifts observed and calculated for the O_3-D_2O and O_3-HDO complexes are listed in Table 5. Frequency shifts of ozone bands are essentially the same in the case of the O_3-H_2O complex. For the D_2O bands, our calculation predicts that asymmetric and symmetric stretching frequencies red shift ($\Delta\nu_1 = -5$ and $\Delta\nu_3 = -6$ cm^{-1}), while the bending frequency blue shifts ($\Delta\nu_2 = +9$ cm^{-1}). The observed shifts for the D_2O vibrations are $\Delta\nu_1 = -0.4$ cm^{-1}, $\Delta\nu_2 = +2$ cm^{-1}, and $\Delta\nu_3 = -5$ cm^{-1}. The HDO asymmetric and symmetric stretching frequencies are calculated to be red shifted ($\Delta\nu_1 = -6$ and $\Delta\nu_3 = -9$ cm^{-1}), while the bending frequency blue shifts ($\Delta\nu_2 = +12$ cm^{-1}). The observed shifts for the HDO vibrations are $\Delta\nu_1 = -8$ and $\Delta\nu_2 = +2$ cm^{-1}. The present calculations reproduce the observed frequency shifts upon the complexation qualitatively; namely, all of the directions of the band shift (red or blue shift) calculated agree with the observation. The quantitative agreement between calculation and experiment was not obtained, which is partly caused because of the harmonic approximation.

Atmospheric Abundance of the Ozone−Water Complex. Next, we calculate an atmospheric abundance of the ozone−water complex according to the procedures presented by Vaida and Headrick.[24] An atmospheric abundance of the ozone−water complex is expressed by

$$\left(\frac{P_{O_3-H_2O}}{P}\right) = K_p(T)P\left(\frac{P_{O_3}}{P}\right)\left(\frac{P_{H_2O}}{P}\right) \quad (3)$$

where P is the ambient pressure, $P_{O_3-H_2O}$, P_{O_3}, and P_{H_2O} are partial pressures of the corresponding atmospheric species, T is temperature, and $K_p(T)$ is the pressure- and temperature-dependent equilibrium constant for complexation. $K_p(T)$ is related to the Gibb's free energy change of

$$\Delta G^\circ = \Delta H^\circ - T\Delta S^\circ \quad (4)$$

by

$$K_p(T)P = \exp(-\Delta G^\circ/RT) \quad (5)$$

where R is the universal gas constant. Thus, we need to know the ΔH° and ΔS° values of the complexation.

TABLE 6: Data Used for Atmospheric Abundance Estimation[a]

	vibrational frequencies (cm^{-1})	rotational constants (cm^{-1})	binding energy (D_e, kcal/mol)	symmetry number (σ)	degeneracy (g_e)
O_3	1103[b], 1042[b], 709[b]	3.5534[b], 0.44525[b], 0.39479[b]		2	1
H_2O	3942[c], 3832[c], 1648[c]	27.877[b], 14.512[b], 9.285[b]		2	1
O_3-H_2O	3911[d], 3806[d], 1645[d], 1110[e], 1045[e], 703[e], 246[f], 140[f], 70[g], 56[f], 53[f], 50[f]	0.384[h], 0.148[h], 0.115[h]	1.89[i]	1	1

[a] Most values exept for the rotational constants and some vibrational frequencis of the O_3-H_2O complex are taken from ref 2 with specific reference given in footnotes b−d, f, and g. [b] Taken from ref 23. [c] Taken from ref 25. [d] Reference 13, scaled to harmonic value following ref 25. [e] This work. [f] Intermolecular vibrational frequencies of water dimer (ref 25) was scaled for ozone−water complex by referencing to the experimentally determined stretching vibration of 70 cm^{-1} (ref 7). [g] Taken from ref 7. [h] This work, the "double-decker conformer" calculated at CCSD(T)/6-311++G(d,p). [i] This work, calculated at CCSD(T)/6-311++G(3df,3pd)//CCSD(T)/6-311++G(d,p) with counterpoise correction for energy calculation.

The enthalpy change of $\Delta H°$ is given by

$$\Delta H° = -4RT + \Delta E_{vib} - D_e \quad (6)$$

where ΔE_{vib} is the change in the vibrational contribution to internal energy upon complexation and D_e is the binding energy of the ozone−water complex. ΔE_{vib} can be calculated by

$$\Delta E_{vib} = E_{vib}(O_3 - H_2O) - [E_{vib}(O_3) + E_{vib}(H_2O)] \quad (7)$$

The individual $E_{vib}(x)$ is given by

$$E_{vib} = \frac{hcR}{k_B}\sum_{j=1}^{3n-6}\left\{\tilde{\nu}_j\left[\frac{1}{2} + (e^{(hc\tilde{\nu}_j/k_BT)} - 1)^{-1}\right]\right\} \quad (8)$$

where h is Plank's constant, c is the speed of light in vacuum, k_B is Boltzman's constant, n is the number of atoms in the molecule, and $\tilde{\nu}_j$ is the jth vibrational frequency in wavenumbers.

The entropy change for complexation, $\Delta S°$, is expressed by

$$\Delta S° = \Delta S_{trans} + \Delta S_{rot} + \Delta S_{vib} + \Delta S_{elec} \quad (9)$$

where the four ΔS_x (x = trans, rot, vib, and elec) terms correspond to the entropy changes caused by translational, rotational, vibrational, and electronic contributions, respectively. The ΔS_x values can be written by

$$\Delta S_x = S_x(O_3 - H_2O) - [S_x(O_3) + S_x(H_2O)] \quad (10)$$

The individual terms of ΔS_x are calculated by using vibrational frequencies and rotational constants of monomers and the complex and are expressed as follows:

$$S_{trans} = R\ln\left[\left(\frac{2\pi m k_B T}{h^2}\right)^{3/2}\cdot\frac{e^{5/2}k_BT}{P}\right] \quad (11)$$

$$S_{rot} = R\ln\left[\left(\frac{T^3}{h^3c^3\theta_A\theta_B\theta_C}\right)^{1/2}\cdot\frac{\pi^{1/2}e^{3/2}}{\sigma}\right] \quad (12)$$

$$S_{vib} = R\sum_{j=1}^{3n-6}\left\{\frac{hc\tilde{\nu}_j}{k_BT}\cdot(e^{(hc\tilde{\nu}_j/k_BT)} - 1)^{-1} - \ln(1 - e^{(hc\tilde{\nu}_j/k_BT)})\right\} \quad (13)$$

$$S_{elec} = R\ln g_e \quad (14)$$

where m is the mass of the molecule, σ is the molecular symmetry number, θ_x (x = A, B, C) are rotational constants in wavenumbers, and g_e is the molecular ground-state degeneracy.

Table 6 summarizes data used for calculation. Frequencies of intermolecular modes of the O_3-H_2O complex are estimated from those of the water dimer. With the binding energy of 1.89 kcal/mol, $K_p(T)$ under the conditions of P = 1 atm and T = 298 K was estimated to be 1.38×10^{-3} atm^{-1}. This value lies in a range of 2×10^{-4} to 4×10^{-3} atm^{-1} calculated by Frost and Vaida,[2] who used the estimated binding energies between 0.7 and 2.4 kcal/mol. We can simply estimate the concentration of the ozone−water complex at the surface of Earth using the $K_{P=1\ atm}^{O_3-H_2O}$ (T = 298 K) = 1.38×10^{-3} atm^{-1} under the following conditions as temperature of 298 K, pressure of 1 atm, tropospheric ozone concentration of 50 ppb, and relative humidity of 50%. The equilibrium ozone−water complex concentration was derived to be 2.0 ppt, which means that 0.004% of ozone may exist as the water complex. It might be noted here that the $K_P(T)$ value depends on the low frequencies of intermolecular modes within the complex. The $K_{P=1atm}^{O_3-H_2O}(T = 298\ K)$ value becomes 1.7×10^{-4} atm^{-1} if one uses calculated low frequencies of 214, 166, 132, 93, 90, and 69 cm^{-1} (listed in Table 2) instead of intermolecular vibrational frequencies of 246, 140, 70, 56, 53, and 50 cm^{-1} (listed in Table 6) employed for the present calculation.

The equilibrium constant calculated for water dimerization was reported in several papers.[24,26−29] Slanina et al. calculated the $K_{P=1atm}^{H_2O-H_2O}(T = 298\ K)$ of 4.5×10^{-2} atm^{-1}, using a simple harmonic potential to describe the vibrations of the water dimer.[26] More recently, Goldman et al. reported the value of $K_{P=1atm}^{H_2O-H_2O}(T = 298\ K)$ of 7.3×10^{-2} atm^{-1} (read from Figure 1 of ref 28) using a more sophisticated intermolecular potential of water dimer, VRT(ASP-W)III.[28] The $K_P(T)$ values of latter authors seems to show reasonable agreement with experimental values reported by Curtiss et al.[30] For the O_2-H_2O complex, Sabu et al.[31] calculated the equilibrium constant of $K_{P=1atm}^{O_2-H_2O}(T = 300\ K) = 4.1 \times 10^{-5}$ atm^{-1}, which is much smaller than the value of 4.3×10^{-3} atm^{-1} reported by Kjaergaard et al.[32] The former authors employed an anharmonic potential to describe the intermolecular O_2-H_2O vibration, while the latter used the harmonic one.

Three molecular complexes of O_2-H_2O, O_3-H_2O, and H_2O-H_2O are extremely floppy species, the binding energies of which are 0.5, 1.9, and ~5.0 kcal/mol, respectively. For a more sophisticated estimation for the $K_P(T)$ value, the precise analyses of the low-frequency intermolecular vibrations of the O_3-H_2O complex are required for experiment and theory.

For the purpose of understanding the atmospheric importance of the O_3-H_2O complex as an OH radical source, there still remains a few uncertain quantities to be determined: (1) a more accurate $K_P(T)$ value or atmospheric abundance ($P_{O_3-H_2O}/P$), (2) the absorption cross section of the O_3-H_2O complex in the UV region of 310−360 nm, the solar radiation of which is strong in the lower troposphere, (3) the $O(^1D)$ yield from the photolysis of the O_3-H_2O complex, and (4) the OH radical yield from the photochemical reaction within the complex.

Conclusions

The ozone−water complex isolated in a cryogenic neon matrix was identified. Infrared absorption due to the complex was assigned in ozone asymmetric stretching, bending, symmetric stretching, and water bending frequency regions. The water symmetric stretching band within the complex was observed between the bands due to the water nonrotating monomer and the proton-acceptor of the water dimer. This result indicates that the ozone−water complex does not have a hydrogen-bonded configuration. The D_2O symmetric and asymmetric stretching bands within the O_3-D_2O complex and the HDO symmetric stretching band within the O_3−HDO complex were also identified.

The geometry optimizations were performed at the MP4-(SDQ), QCISD, and CCSD(T) levels with a 6-311++G(d,p) basis set. Only one conformer, which was named "double-decker", was found to be stable. Frequencies of the "double-decker" conformer calculated at the CCSD(T)/6-311++G(d,p) level of theory was compared with the experimentally observed vibrational frequencies. Our calculation reproduces the direction of the band shift (red or blue shift) for all of the observed vibrations within the complex.

By using statistical thermodynamics, monomer and complex vibrational frequencies/rotational constants, and the binding energy of the complex, we calculated the change of enthalpy and entropy upon the complexation. From these values, the equilibrium constant was derived, and the atmospheric abundance of the ozone−water complex was estimated at Earth's surface level.

Acknowledgment. The present work is partly defrayed by the Grant-in-Aid for Scientific Research (No. 17350005) and by the Grant-in-Aid for Scientific Research on Priority Areas (B) (No. 13127202) from the Ministry of Education, Culture, Sports, Science and Technology, Japan.

Supporting Information Available: Infrared absorption spectra in the D_2O symmetric/asymmetric stretching and the HDO symmetric stretching frequency regions. This material is available free of charge via the Internet at http://pubs.acs.org.

References and Notes

(1) Matsumi, Y; Kawasaki, M. *Chem. Rev.* **2003**, *103*, 4767.
(2) Frost, G. J.; Vaida, V. *J. Geophys. Res.* **1995**, *100*, 18803.
(3) Staikova, M.; Donaldson, D. J. *Phys. Chem. Earth, Part C: Solar−Terrestrial & Planetary Science* **2001**, *26*, 473.
(4) Hurwitz, Y.; Naaman, R. *J. Chem. Phys.* **1995**, *102*, 1941.
(5) Vaida, V.; Frost, G. J.; Brown, L. A.; Naaman, R.; Hurwitz, Y. *Ber. Bunsenges. Phys. Chem.* **1995**, *99*, 371.
(6) Zakharov, I. I.; Kolbasina, O. I.; Semenyuk, T. N.; Tyupalo, N. F.; Zhidomirov, G. M. *J. Struct. Chem.* **1993**, *34*, 359.
(7) Gillies, J. Z.; Gillies, C. W.; Suenram, R. D.; Lovas, F. J.; Schmidt, T.; Cremer, D. *J. Mol. Spectrosc.* **1991**, *146*, 493.
(8) Tachikawa, H.; Abe, S. *Inorg. Chem.* **2003**, *42*, 2188.
(9) Schriver-Mazzuoli, L; Schriver, A.; Lugez, C.; Perrin, A.; Camy-Peyret, C.; Flaud, J.-M. *J. Mol. Spectrosc.* **1996**, *176*, 85.
(10) Brosset, P.; Dahoo, R.; Gauthier-Roy, B.; Abouaf-Marguin, L.; Lakhlifi, A. *Chem. Phys.* **1993**, *172*, 315.
(11) Raducu, V.; Jasmin, D.; Dahoo, R.; Brosset, P.; Gauthier-Roy, B.; Abouaf-Marguin, L. *J. Chem. Phys.* **1994**, *101*, 1878.
(12) Frei, H.; Fredin, L.; Pimentel, G. C. *J. Chem. Phys.* **1981**, *74*, 397.
(13) Schriver, L.; Barreau, C.; Schriver, A. *Chem. Phys.* **1990**, *140*, 429.
(14) Frisch, M. J.; Trucks, G. W.; Schlegel, H. B.; Scuseria, G. E.; Robb, M. A.; Cheeseman, J. R.; Montgomery, J. A., Jr.; Vreven, T.; Kudin, K. N.; Burant, J. C.; Millam, J. M.; Iyengar, S. S.; Tomasi, J.; Barone, V.; Mennucci, B.; Cossi, M.; Scalmani, G.; Rega, N.; Petersson, G. A.; Nakatsuji, H.; Hada, M.; Ehara, M.; Toyota, K.; Fukuda, R.; Hasegawa, J.; Ishida, M.; Nakajima, T.; Honda, Y.; Kitao, O.; Nakai, H.; Klene, M.; Li, X.; Knox, J. E.; Hratchian, H. P.; Cross, J. B.; Bakken, V.; Adamo, C.; Jaramillo, J.; Gomperts, R.; Stratmann, R. E.; Yazyev, O.; Austin, A. J.; Cammi, R.; Pomelli, C.; Ochterski, J. W.; Ayala, P. Y.; Morokuma, K.; Voth, G. A.; Salvador, P.; Dannenberg, J. J.; Zakrzewski, V. G.; Dapprich, S.; Daniels, A. D.; Strain, M. C.; Farkas, O.; Malick, D. K.; Rabuck, A. D.; Raghavachari, K.; Foresman, J. B.; Ortiz, J. V.; Cui, Q.; Baboul, A. G.; Clifford, S.; Cioslowski, J.; Stefanov, B. B.; Liu, G.; Liashenko, A.; Piskorz, P.; Komaromi, I.; Martin, R. L.; Fox, D. J.; Keith, T.; Al-Laham, M. A.; Peng, C. Y.; Nanayakkara, A.; Challacombe, M.; Gill, P. M. W.; Johnson, B.; Chen, W.; Wong, M. W.; Gonzalez, C.; Pople, J. A. *Gaussian 03*, revision C.02; Gaussian, Inc.: Wallingford, CT, 2004.
(15) Simon, S.; Duran, M.; Dannenberg, J. J. *J. Chem. Phys.* **1996**, *105*, 11024.
(16) Winn, J. S. *J. Chem. Phys.* **1991**, *94*, 5275.
(17) Lang, V. I.; Winn, J. S. *J. Chem. Phys.* **1991**, *94*, 5270.
(18) Forney, D.; Jacox, M. E.; Thompson, W. E. *J. Mol. Spectrosc.* **1993**, *157*, 479.
(19) Bouteiller, Y.; Perchard, J. P. *Chem. Phys.* **2004**, *305*, 1.
(20) Suma, K; Sumiyoshi, Y; Endo, Y. *Science* **2006**, *311*, 1278.
(21) Kasai, Y.; Sumiyoshi, Y.; Endo, Y. Presented at the 55th International Symposium on Molecular Spectroscopy, The Ohio State University Columbus, OH, 2000.
(22) Sabu, A.; Kondo, S.; Miura, N.; Hashimoto, K. *Chem. Phys. Lett.* **2004**, *391*, 101.
(23) Herzberg, G. *Molecular Spectra and Molecular Structure: III. Electronic Spectra and Electronic Structure of Polyatomic Molecules*; Krieger Publishing Company: Malabar, FL, 1991.
(24) Vaida, V.; Headrick, J. E. *J. Phys. Chem. A* **2000**, *104*, 5401.
(25) Kim, K. S.; Mhin, B. J.; Choi, U.; Lee, K. *J. Chem. Phys.* **1992**, *97*, 6649.
(26) Slanina, Z.; Crifo, J. F. *Int. J. Thermophys.* **1992**, *13*, 465.
(27) Goldman, N.; Fellers, R. S.; Leforestier, C.; Saykally, R. J. *J. Phys. Chem. A* **2001**, *105*, 515.
(28) Goldman, N.; Fellers, R. S.; Brown, M. G.; Braly, L. B.; Keoshian, C. J.; Leforestier, C.; Saykally, R. J. *J. Chem. Phys.* **2002**, *116*, 10148.
(29) Cheunter, G. K.; Kathmann, S. M.; Garrett, B. C. *J. Phys. Chem. A* **2002**, *106*, 1557.
(30) Curtiss, L. A.; Frurip, D. J.; Blander, M. *J. Chem. Phys.* **1979**, *71*, 2703.
(31) Sabu, A.; Kondo, S.; Saito, R.; Kasai, Y.; Hashimoto, K. *J. Phys. Chem. A* **2005**, *109*, 1836.
(32) Kjaergaard, H. G.; Robinson, T. W.; Howard, D. L.; Daniel, J. S.; Headrick, J. E.; Vaida, V. *J. Phys. Chem. A* **2003**, *107*, 10680.